Microstructured optical fibers: where's the edge?

Boris T. Kuhlmey

School of Physics, University of Sydney, NSW 2006, Australia
and Institut Fresnel, Unité Mixte de Recherche du Centre National pour la Recherche Scientifique 6133, Faculté des Sciences et Techniques de St Jérôme, 13397 Marseille Cedex 20, France
borisk@physics.usyd.edu.au

Ross C. McPhedran, C. Martijn de Sterke and Peter A. Robinson

School of Physics, University of Sydney, NSW 2006, Australia
ross@physics.usyd.edu.au, desterke@physics.usyd.edu.au, p.robinson@physics.usyd.edu.au

Gilles Renversez and Daniel Maystre

Institut Fresnel, Unité Mixte de Recherche du Centre National pour la Recherche Scientifique 6133, Faculté des Sciences et Techniques de St Jérôme, 13397 Marseille Cedex 20, France
gilles.renversez@fresnel.fr, daniel.maystre@fresnel.fr

Abstract: We establish that Microstructured Optical Fibers (MOFs) have a fundamental mode cutoff, marking the transition between modal confinement and non-confinement, and give insight into the nature of this transition through two asymptotic models that provide a mapping to conventional fibers. A small parameter space region where neither of these asymptotic models holds exists for the fundamental mode but not for the second mode; we show that designs exploiting unique MOF characteristics tend to concentrate in this preferred region.

OCIS codes: (060.2430) Fibers, single-mode; (060.2270) Fiber characterization; (060.2280) Fiber design and fabrication; (230.3990) Microstructure devices

References and Links

1. R. F. Cregan, B. J. Mangan, J. C. Knight, T. A. Birks, P.S. Russel, P. J. Roberts, D. C. Allan, "Single-mode photonic band gap guidance of light in air," Science **285**, 1537-1539 (1999).
2. T. M. Monro, D. J. Richardson, N. G. R. Broderick, P. J. Bennett, "Holey optical fibers: An efficient modal model," J. Lightwave Technol. **17**, 1093-1102 (1999).
3. J. K. Ranka, R. S. Windeler, A. J. Stentz, "Visible continuum generation in air-silica microstructure optical fibers with anomalous dispersion at 800 nm," Opt. Lett. **25**, 25-27 (2000).
4. A. Ferrando, E. Silvestre, J. J. Miret, P. Andrés, "Nearly zero ultraflattened dispersion in photonic crystal fibers," Opt. Lett. **25**, 790-792 (2000).
5. J. C. Knight, J. Arriaga, T. A. Birks, A. Ortigosa-Blanch, W. J. Wadsworth, P. S. Russell, "Anomalous dispersion in photonic crystal fiber," IEEE Photonic Tech. Lett. **12**, 807-809 (2000).
6. W. H. Reeves, J. C. Knight, P. St. J. Russell,"Demonstration of ultra-flattened dispersion in photonic crystal fibers," Opt. Express **10**, 609-613 (2002), http://www.opticsexpress.org/abstract.cfm?URI=OPEX-10-14-609.
7. B. Kuhlmey, G. Renversez, D. Maystre, "Chromatic dispersion and losses of microstructured optical fibers," Appl. Optics OT, in press.
8. T. A. Birks, J. C. Knight, P. St. Russell, "Endlessly single-mode photonic crystal fiber," Opt. Lett. **22**, 961-963 (1997).
9. J. C. Knight, T. A. Birks, R. F. Cregan, P. St. Russell, J. P. de Sandro, "Large mode area photonic crystal fibre," Electron. Lett. **34**, 1347-1348 (1998).
10. R. Holzwarth, M. Zimmermann, Th. Udem, T. W. Hänsch, P. Russbüldt, K. Gäbel, R. Poprawe, J. C. Knight, W. J. Wadsworth, P. St. J. Russell, "White-light frequency comb generation with a diode-pumped Cr:LiSAF laser," Opt. Lett. **26**, 1376-1378 (2001)

#1676 - $15.00 US Received September 28, 2002; Revised October 25, 2002

11. A. V. Husakou, J. Herrmann, "Supercontinuum Generation of Higher-Order Solitons by Fission in Photonic Crystal Fibers," Phys. Rev. Lett. **87**, 203901 (2001).
12. J. P. Dudley, L. Provino, N. Grossard, H. Maillotte, R. S. Windeler B. J. Eggleton, S. Coen, "Supercontinuum generation in air–silica microstructured fibers with nanosecond and femtosecond pulse pumping," J. Opt. Soc. Am. B **19**, 765-771 (2002).
13. T. P. White, B. T. Kuhlmey, R. C. McPhedran, D. Maystre, G. Renversez, C. M. de Sterke, L. C. Botten, "Multipole method for microstructured optical fibers. I. Formulation," J. Opt. Soc. Am. B **19**, 2322-2330 (2002).
14. B. T. Kuhlmey, T. P. White, R. C. McPhedran, D. Maystre, G. Renversez, C. M. de Sterke, L. C. Botten, "Multipole method for microstructured optical fibers. II. Implementation and results," J. Opt. Soc. Am. B **19**, 2331-2340 (2002).
15. T. P. White, R. C. McPhedran, C. M. de Sterke, M. J. Steel, "Confinement losses in microstructured optical fibers," Opt. Lett. **26**, 1660-1662 (2001).
16. N. A. Mortensen, "Effective area of photonic crystal fibers," Opt. Express **10**, 341-348 (2002), http://www.opticsexpress.org/abstract.cfm?URI=OPEX-10-7-341.
17. B. T. Kuhlmey, R. C. McPhedran, C. M. de Sterke, "Modal 'cutoff' in Microstructured Optical Fibers," Opt. Lett. **27**, 1684-1686 (2002).
18. G. W. Milton, *The Theory of Composites* (Cambridge University Press, 2002).
19. A. W. Snyder, J. D. Love, *Optical Waveguide Theory* (Chapman & Hall, London, 1996).
20. J. C. Knight, T. A. Birks, P. St. Russell, J. P. de Sandro, "Properties of photonic crystal fiber and the effective index model," J. Opt. Soc. Am. B **15**, 748-752 (1998).
21. F. Brechet, J. Marcou, D. Pagnoux, P. Roy, "Complete analysis of the characteristics of propagation into photonic crystal fibers, by the finite element method," Opt. Fiber Technol. **6**, 181-191 (2000).
22. T. Monro, P. J. Bennett, N. G. Broderick, D. J. Richardson, "Holey fibers with random cladding distributions," Opt. Lett. **25**, 206-208 (2000).

Microstructured Optical Fibers (MOFs) have received considerable attention since pioneering work demonstrated some of their remarkable properties, such as guidance in hollow cores [1], unprecedented dispersion characteristics [2-7], "endlessly" single-modedness [8], and the support of modes with extremely low or high effective area [2,9]. These unique properties have far-reaching consequences in fundamental and applied areas as diverse as frequency comb generation [10], supercontinuum generation [3,11,12] and dispersion management [5].

One of the most important MOF configurations consists of a silica fiber with a solid core surrounded by a silica cladding pierced by rings of air holes, that are typically hexagonally packed (Fig. 1, lower right inset). These holes can be thought of as acting to depress the average cladding refractive index, so that light escaping the core has to tunnel through an equivalent low-index layer. An intriguing difference between such MOFs and conventional fibers is associated with the distinction between guided and non-guided modes. In conventional fibers the distinction is clear-cut: guided modes are lossless and thus have real propagation constants β, related to a real effective index n_{eff} by $n_{\mathrm{eff}} = \beta/k_0 = 2\pi\beta/\lambda$, where λ and k_0 are the light's wavelength and vacuum wavenumber, respectively. For non-guided modes β and n_{eff} are complex, where the imaginary part of n_{eff} is linearly related to the loss coefficient at fixed wavelength. In MOFs with a finite number N_r of rings of confining holes, all modes can tunnel through the confinement region to some extent and are consequently lossy; thus all modes have complex values of β and n_{eff} [13-15].

In two recent papers [16,17] criteria were established for recognizing the transition of the second mode[1] from being unconfined to confined, which we identify with cutoff. Mortensen [16] used the rapid decrease in the mode's effective area at the transition, whereas Kuhlmey *et al.* [17] used effective area and four other criteria to pinpoint the transition. Curve 3 in Fig. 1 shows the locus of the transition of the second mode as a function of wavelength normalized to hole spacing Λ, for MOFs of various hole diameters d in silica. Note that this curve crosses the horizontal axis at d/Λ=0.406. Though the transition is gradual for MOFs with only a few rings of air holes, it becomes sharper when the number of air holes increases [17].

[1] The second mode is defined as the mode having, for a given fiber geometry, the second largest real part of n_{eff}. It usually has the second lowest loss, and its field distribution is similar to the TE_1 mode of conventional fibers.

#1676 - $15.00 US Received September 28, 2002; Revised October 25, 2002

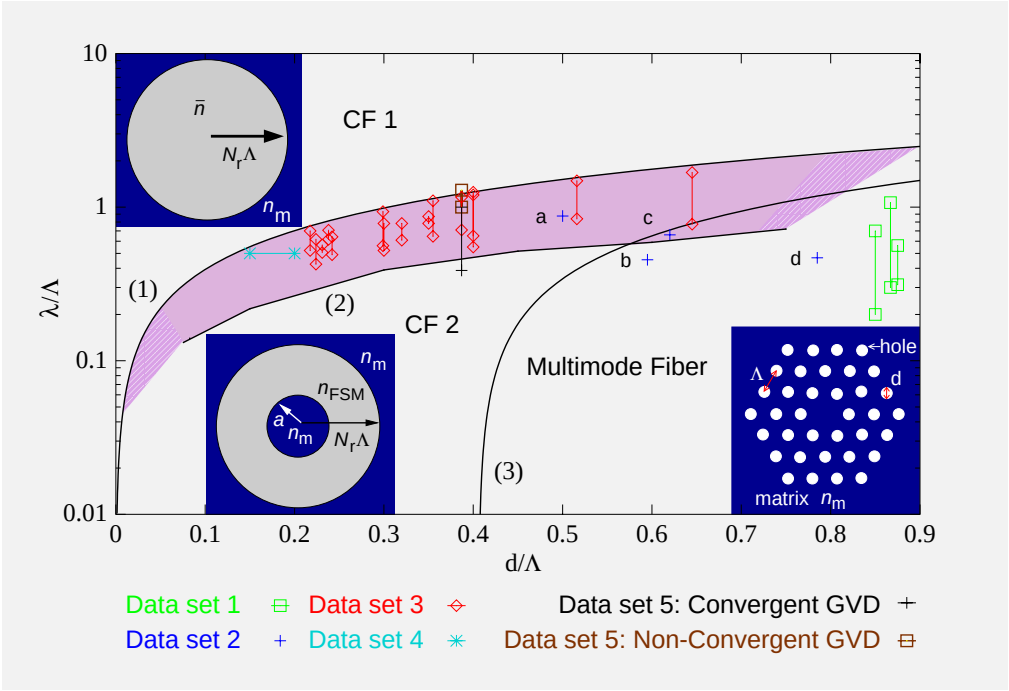

Fig. 1. Operation regimes of MOFs. Lower right inset: cross section of a MOF with 3 rings of holes. Other insets: asymptotic models for large (CF1) and small (CF2) wavelengths. The shaded transition region represents the parameter subspace where MOFs cannot be described by either asymptotic model and therefore behave most unlike conventional optical fibers. Data sets are described in the text.

Using the same criteria as in [17], it appears that the fundamental mode[2] also undergoes a cutoff transition between confined and non-confined states. For long wavelengths, the fundamental mode fills the entire fiber cross-section, whereas for small wavelength it becomes confined in the core. However, instead of having the sharp transition between those states exhibited by the second mode, the transition is characterized by two loci, with a transition region of finite width in between. This was established for structures of up to N_r=10 rings of holes, with conclusions for larger structures following by extrapolation . Above the highest of these loci [curve (1)], in the region denoted by CF1, the fundamental mode fills the entire fiber cross section, and its properties can be accurately predicted on the basis of a conventional fiber model (CF1, using the same symbol for the model and the region of parameter space in which it is valid) that we describe below. Below the second locus [curve (2)], in the region denoted by CF2, the fundamental mode is tightly confined in the core, with its properties given by a second conventional fiber model (CF2). In the transition region between CF1 and CF2, the fundamental mode changes its character and its behavior is thus not only sensitive to the MOF design (*i.e.*, to d/Λ and N_r), but is also unlike that of the modes of conventional fibers. We stress that, as we decrease the wavelength from large values, the fiber at first shows no localized modes (region CF1), but that one of its extended modes undergoes a smooth transition to emerge as a localized mode in region CF2.

We established the mode boundaries of Fig. 1 using a multipole method [13,14], which can calculate MOF modes and their losses accurately over a wide parameter range. We studied the comportment of MOFs at the telecommunications wavelength of λ=1.55 μm, and varied the hole spacing Λ, while keeping the hole diameter to spacing ratio d/Λ constant. The

[2] The fundamental mode is defined as the mode having, for a given fiber geometry, the largest real part of n_{eff}. It is the mode with the lowest losses and for the fibers studied here is doubly degenerate. It is most similar in terms of field distribution to the $HE_{1,1}$ mode of conventional fibers.

#1676 - $15.00 US
Received September 28, 2002; Revised October 25, 2002

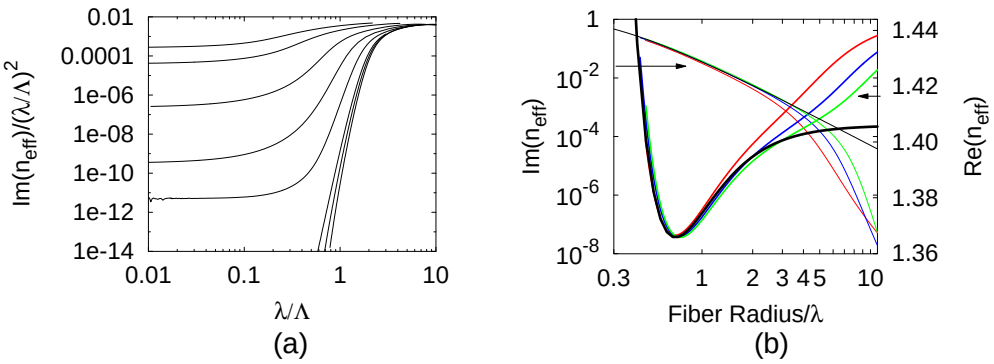

Fig. 2. **A**: Imaginary part of n_{eff} as a function of wavelength on pitch, rescaled by $(\lambda/\Lambda)^2$, for a silica structure with 3 layers of holes, with d/Λ taking the values 0.075 (top curve), 0.15, 0.3, 0.45, 0.6, 0.75, 0.8 and 0.85. **B**: Imaginary (thin curves) and real (thick curves) part of n_{eff} as a function of fiber radius $N_r\Lambda$ divided by λ for MOFs with d/Λ=0.3, for 4 (red), 6 (blue) and 8 (green) rings of holes, and for the corresponding homogenized fiber (black). All calculations in this report were done for varying pitch at fixed λ=1.55μm, where the losses in dB/m are given by $3.52\text{x}10^7\text{Im}(n_{eff})$.

MOFs were taken to consist of air holes (refractive index unity) in a matrix with refractive index n_m=1.44402362. For given d/Λ, we studied the variation of the loss [Im(n_{eff})] as a function of normalized wavelength λ/Λ. At small λ/Λ, the loss increases gently, before rising very steeply in the transition region, and then increasing slowly once again in the second conventional fiber region (see Fig. 2.A). To locate the boundaries of regions accurately, we used the second derivative of the log-log plot of the losses, a function which peaks at the boundaries between regions [17]. Carrying out this procedure for various hole diameters, we established the two boundary curves for the fundamental mode, shown for the first time in Fig. 1. These curves tend to approach one another for decreasing hole size, and reach λ=0 for hole sizes d/Λ somewhere between 0 and 0.06 inclusive. Counting only modes confined to the core, MOFs in silica can be said to be "endlessly" single-moded in the region below the CF1 area of Fig. 1, and to the left of d/Λ = 0.406, where the second mode boundary drops to zero [17]. This observation corroborates and somewhat sharpens the prediction of endless single mode behavior made by Birks *et al.* [8].

In the CF1 region of Fig.1, the fundamental mode fills the entire confining region. Its behavior is modeled accurately by using homogenization arguments [18] to establish effective dielectric constants and thereby refractive indices for the cladding region. Homogenization theory predicts an effective dielectric constant given by the mean of the dielectric constants of air and silica for the electric field parallel to the fiber axis. In contrast, for small d/Λ the Maxwell-Garnett formula can be used to derive effective constants for the transverse electric field component [18]. With f being the air filling fraction of the fiber we have:

$$\bar{n}_z = \left[f\, n_{air}^2 + (1-f)\, n_m^2\right]^{1/2}, \qquad \text{(Extraordinary index)} \qquad (1)$$

$$\bar{n}_\perp \cong n_m\left[(T-f)/(T+f)\right]^{1/2}, \qquad \text{(Ordinary index)} \qquad (2)$$

$$\text{where } T = (n_m^2 + n_{air}^2)/(n_m^2 - n_{air}^2).$$

The effective modal index is then calculated using the theory [19] of propagation in an optical fiber with core of radius $N_r\Lambda$ constituting a uniaxial material, and a silica jacket. Fig. 2.B shows the real and imaginary parts of the effective index of a MOF for different numbers of rings as a function of the fiber size $N_r\Lambda$ and the results given by the homogenized model outlined above. The agreement is excellent for $\lambda/\Lambda \geq 0.5$. Thus in this regime the mode properties remarkably only depend on the total fiber size $N_r\Lambda$, regardless of N_r. MOF modes

#1676 - $15.00 US
Received September 28, 2002; Revised October 25, 2002

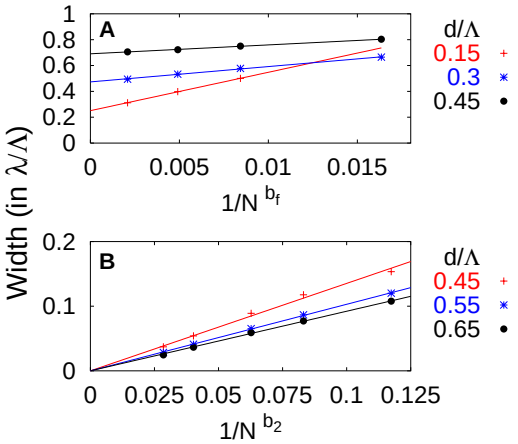

Figure 3: Width of the transition between the large wavelength asymptotic regime (CF1) and the intermediate regime as a function of N_r^{-b}, for the fundamental mode (A, $b_f \approx 2.97$) and the second mode (B, $b_2 \approx 1.55$). For the second mode the width of the intermediate regime tends to zero with increasing number of rings, whereas a finite transition region remains for the fundamental mode, even for $N_r \to \infty$.

tend to be quite lossy here, since the effective indices in the core region are smaller than n_m. Note that the losses do decrease as the number N_r of layers of confining air holes increases, but do so following a power law. Consequently, N_r generally has to be impractically large to generate MOFs with sufficiently low loss for technological applications, and key quantities like the modal dispersion depend sensitively on N_r, even when this number is large. Therefore, practical applications of MOFs are unlikely for designs in the CF1 region of Fig. 1.

For short wavelengths, MOFs have already been successfully modeled by several authors as step index fibers with varying cladding index [5,8,11,12,20,21]. In the model CF2 shown in Fig. 1 the refractive index of the cladding is given by the effective index of the fundamental space-filling mode (FSM) [8]. Best agreement was found for a core radius of approximately $a=0.64\Lambda$ [21]. Based on an asymptotic analysis of this model, it appears that at short wavelengths n_{FSM} can be approximated by

$$n_{FSM} = n_m - n_2(\lambda/\Lambda)^2 \qquad (3)$$

where n_2 can be obtained from a transcendental equation derived from the framework established by Birks *et al.* [8]. It is then readily shown that the imaginary part of the effective index varies as $(\lambda/\Lambda)^2$ for a fixed number N_r of rings of air holes, and decays exponentially with N_r at fixed $k_0\Lambda$, as expected for tunneling losses. Fig. 2.A shows the imaginary part of n_{eff} divided by $(\lambda/\Lambda)^2$ as a function of λ/Λ, for several d/Λ ratios. The curves tend to a constant for approximately $\lambda/\Lambda \leq 0.3$, indicating clearly that the asymptotic dependence becomes valid for reasonable wavelength to pitch ratios. In this regime, and contrary to the behavior in the CF1 regime, the real part of n_{eff}, and derived characteristics such as modal dispersion converge with increasing N_r.[3]

It is thus clear that the region CF2 of Fig. 1 is appropriate for practical MOF designs: Confinement of the fundamental mode improves exponentially as more rings are added, and characteristics such as modal dispersion converge with an increasing number of rings. However, the further the CF2 region is penetrated, the closer the analogy becomes between the MOF and conventional fibers. Thus, the new design possibilities offered by MOFs are essentially available only in the transition region and its border with the region CF2.

[3] Note that n_{FSM} also has importance in relation to the boundary of CF1, which appears to occur when $n_{eff} = n_{FSM}$.

#1676 - $15.00 US Received September 28, 2002; Revised October 25, 2002

As mentioned earlier, the sharpness of the transition region with increasing N_r evolves differently for the fundamental and the second mode. This is illustrated in Fig. 3, where we plot the width of the transition region (more precisely the width of the peak of the second derivatives of the curves in Fig. 1.A) versus $1/N_r^b$, where b is adjusted to give the best straight-line behavior of all datasets in each frame. As the number of confining rings N_r increases, the width of the transition region tends to zero for the second mode (Fig. 3.B), whereas for the fundamental mode this width remains finite (Fig. 3.A). Thus, in an infinite system, the transition region for the second mode disappears, whereas for the fundamental mode there is always a parameter region in which this mode behaves fundamentally differently than the modes of a conventional fiber. Note the linearity of the data for different hole diameters in Fig. 3, showing that the power law exponents for both modes are independent of d/Λ.

The points in Fig. 1 indicate experimental and theoretical data from recent publications of MOF designs with unconventional properties. The first data set concerns MOFs used experimentally for supercontinuum generation, taken from Refs. [3,11-12]. They all lie in the CF2 regime, and indeed the key property for supercontinuum generation – highly shifted zero dispersion wavelength and small core size – can be delivered by the CF2 model, already known to be successful for such MOFs [11,12]. Data set 2 shows the location of experimental zero-dispersion wavelength measures, which were compared to theoretical values from a CF2 model in the original publication [5]. For the two lower points (b and d) which lie in the CF2 region, comparison with the CF2 model gave good agreement, for point c agreement was approximate and for point a, lying in the transition region, the agreement was unsatisfactory.

The third data set consists of regions of observed or predicted flat or oscillating dispersion, taken from Refs. [2,4,6,7,21]. All data points herein are located exactly in the transition region, using the increased and highly configurable wavelength dependence of structural dispersion to compensate material dispersion. The consequences of being in the transition region, and therefore close to cutoff, are that confinement losses are highly wavelength dependent, and that the waveguide dispersion is sensitive to the actual fiber geometry. Such high sensitivity to structural imperfections was observed by Monro *et al.* [22], and indeed the fiber parameters used by these authors are in the transition region (data line 4).

In studying the influence of the number of rings on dispersion [7], we observed that the dispersion does not necessarily converge with the ring number. Data set 5 shows the location of an example where the dispersion converges with N_r in a limited wavelength range before diverging with N_r. The divergent wavelength range crosses the transition line from the intermediate to the homogenized regime CF1, where we have seen N_r dictates mode properties.

Although we tried to map as many published MOF designs as possible onto Fig. 1, a few were omitted: some were overlapping the transition region and the CF2 region and had more conventional dispersion properties, while others were beyond the scope of this study (*e.g.* grossly non-circular holes). One theoretical study by Monro *et al.* [2] had two examples of MOFs lying in the CF1 region, with both displaying conventional dispersion. It should be emphasized that no experimental MOF has been published with parameters in the CF1 region.

In conclusion, we find that the fundamental MOF mode exhibits a transition between being confined around the core region, and filling the entire (finite) fiber cross-section. Thereby, we have shown that MOFs have an edge in the sense of offering modal characteristics unlike those achievable with conventional fibers when operated in the transition region, shown in Fig. 1. They may deliver useful (albeit conventional) design characteristics in the region CF2, but are unlikely to deliver low-loss and stable secondary characteristics such as dispersion in the region CF1. We have shown that these theoretical insights are in keeping with successful MOF designs from the literature, and we are confident they will prove useful in guiding further innovative applications of this exciting new class of optical fiber.

#1676 - $15.00 US Received September 28, 2002; Revised October 25, 2002